Dalton Transactions

ROYAL SOCIETY OF CHEMISTRY

PAPER

View Article Online
View Journal | View Issue

Cite this: *Dalton Trans.*, 2025, **54**, 14937

Heteroleptic tethered NHC rare earth initiators for the ring opening polymerisation of *rac*-lactide

Joseph W. Walker,[a] Tajrian Chowdhury,[b] Georgina M. Rosair,[a] Joy H. Farnaby,[b] Stephen M. Mansell *[a] and Ruaraidh D. McIntosh *[a]

The importance of catalyst design is shown by the contrasting reactivity of tethered NHC and Tp ligands with rare-earth metal centres highlighting that successful catalyst design is not as simple as linearly combining moieties with known catalytic activity. The heteroleptic fluorenyl-tethered-NHC rare-earth complexes $LnLX_2$ [Ln = Y, La, Ce, Nd; L = $(\eta^5\text{-}C_{13}H_8)C_2H_4N(\kappa\text{-}C)C_2H_2NMe$; X = N'' or Br] were synthesised from $[Ln\{N(SiMe_3)_2\}_3]$ (LnN''_3), with X selected by varying the precursor. Direct addition of LnN''_3 to the fluorene-tethered imidazolium salt LH_2Br proceeded with loss of two equivalents of $HN(SiMe_3)_2$ forming [LnL(N'')Br] complexes; alternatively, initial deprotonation of LH_2Br with ^{n}BuLi or KCH_2Ph prior to addition of LnN''_3 yielded $[LnL(N'')_2]$ complexes. [LnL(N'')Br] [Ln = Ce (**3**), Nd (**4**)] are dimeric through bridging Br ligands whereas $[LnL(N'')_2]$ [Ln = La (**5**), Ce (**6**), Nd (**7**)] are monomeric. These complexes were investigated for their activity and selectivity in the ring opening polymerization (ROP) of *rac*-lactide using benzyl alcohol as a co-initiator, showing high activity with full conversion typically being obtained in under 15 minutes at room temperature. Comparisons with the yttrium amide complex $[Y(Tp)_2(N'')]$ (**8**, Tp = hydrotris(1-pyrazolyl)borate) demonstrated the important role of the fluorenyl-tethered NHC ligand in generating an active catalyst, illustrating that simply having a rare-earth metal centre with a bis(trimethylsilyl)amide group is not enough to generate an effective (pre)catalyst. Finally, we hope to raise awareness that a trace impurity of lactic acid, sometimes present in commercial *rac*-lactide, greatly inhibited ROP and was not easily removed by sublimation or re-crystallisation.

Received 9th June 2025,
Accepted 15th September 2025

DOI: 10.1039/d5dt01352f

rsc.li/dalton

Introduction

Developing bio-derivable and bio-degradable polymers, such as polylactic acid (PLA), as alternatives to crude-oil-based polymers has constituted a major area of research in recent years.[1–6] Reduction of plastic use along with improved processing and disposal of plastic waste is a key area of polymer research. PLA waste is degradable to products such as lactic acid, which themselves may be reusable for further PLA synthesis.[7] Ring-opening polymerisation (ROP) by organometallic complexes has been exploited for a variety of monomers to give better control over polymer properties relative to alternative methods such as polycondensation while also reducing energy requirements.[8] Targeted ligand design and choice of metal centre assist in achieving the desired reactivity for PLA synthesis from the cyclic and bio-derivable monomer lactide (LA).[9]

Commercial PLA synthesis *via* catalysis is dominated by tin octoate [tin(II) 2-ethylhexanoate] which requires elevated temperatures to perform the polymerisation because activity is severely limited at temperatures ≤140 °C, with industry typically performing polymerisations under monomer melt conditions at 180 °C for *ca.* 1 hour.[8,10] Control over polymer properties by tin octoate is generally difficult with polymer polydispersities typically in the region of 1.5.[8,10] Research into new ROP catalysts has thus been of major interest, both to improve the properties of PLA and to reduce the amount of energy required for industrial scale polymerisation reactions. In terms of metal choice, one of the most interesting areas is the rare earth metals.[4,11] While they are less studied than main group and transition metals, rare earth metal cations are highly oxophilic, Lewis acidic, and show a very high binding affinity for the cyclic esters utilised in ROP.[5,12] Combined, these factors result in extremely high rates of polymerisation, with full conversion achievable in under a minute at room temperature.[5] The rare earth metals share the commonality of the +3 oxidation state and $4f^n5d^0$ electronic configuration across the series, but the lanthanide contraction causes a decrease in ionic radii as the atomic number increases, resulting in subtle differences in Lewis acidity and reactivity between the elements.[13–15]

[a]*Institute of Chemical Sciences, Heriot-Watt University, Edinburgh, EH14 4AS, UK. E-mail: S.Mansell@hw.ac.uk, R.McIntosh@hw.ac.uk*
[b]*School of Chemistry, University of Glasgow, Joseph Black Building, Glasgow, G12 8QQ, UK*

One ligand type which has received increasing attention in rare earth chemistry is the fluorenyl (Flu) moiety.[16] This ligand type is related to the well-known cyclopentadienyl (Cp) ligand but features benzannulated rings on two sides of the central 5-membered ring.[17] The electron withdrawal of the extended π-network results in weaker electron donation, giving weaker binding and a greater variety of binding modes to metal centres relative to the analogous Cp complexes.[18,19] The main benefit of this property is related to the indenyl effect where η^5 binding of Flu more easily switches to an η^3 or η^1 mode known as ring slippage, and the rate of reaction of these complexes is in the order $k_{Flu} > k_{Ind} > k_{Cp}$.[20] For transition metals, this leaves a two electron vacancy for substrate binding in catalysis.[19] Functionalisation of Flu allows the formation of chelating mixed donor ligands, for example, with amines[21] or N-heterocyclic carbenes (NHC).[22–25]

NHCs are firmly binding and electron donating ligands which act as strong σ-donors and form stable complexes with metals throughout the periodic table including lanthanides.[26,27] Since their advent, NHC complexes have become indispensable in a variety of catalytic applications, a famous example of which is the second generation Grubbs catalyst.[28–31] Polymerisation is no exception to this trend; transition metals, rare earth metals and main group metals have all been utilised with NHC ligands for the polymerisation of alkenes, while ROP of cyclic esters with transition metals has also been investigated.[32,33] In previous work from the Williams group, it was shown that rare-earth initiators for LA polymerisation have significantly higher rates when electron-donating moieties are utilised, of which NHCs are some of the strongest candidates.[5,34] Rare-earth initiators for the ROP of LA have now covered a very large range of ligand types and span both monomeric and polymeric initiator types.[4] Popular choices typically include multidentate or homoleptic ligand sets as these solve issues observed in catalyst synthesis relating to ligand redistribution reactions. Donor atoms are varied with N and O ligand sets being common as both neutral and anionic moieties in addition to mixed-atom donors where combinations of oxygen, nitrogen or other atoms such as sulfur are bound to the metal centre.[35–38] Neutral carbon-based donors such as NHCs are also growing in popularity as they strongly donate electron density to the metal centres while anionic groups such as Cp and CH_2SiMe_3 have been investigated previously.[39,40] More unusual systems for ROP of LA include divalent lanthanides such as Sm(II) supported by bis(indenyl) ligands and multimetallic lanthanide complexes.[40–42]

Combining the beneficial aspects of fluorenyl and NHC ligands through tethering has been of extensive interest to control redistribution reactions and we have previously used this motif to synthesise new rare-earth complexes.[43] Use of an N-Me substituted NHC tethered to fluorenyl through an ethylene linker has previously been investigated in the literature in the copolymerisation of ethylene and styrene derivatives with a scandium metal centre featuring CH_2SiMe_3 coligands where high activity was observed.[44] Use of alkyl coligands, however, results in very reactive species which may be unsuitable for certain polymerisation experiments. Previous work in the group focused on amide coligands, which while less reactive should result in greater stability for the catalytic species. Complexation with early lanthanides (Ln = Y, La, Nd) was investigated from LnN''_3 precursors. A heteroleptic monomeric Y complex was isolated, while single crystals of a dimeric Nd complex with bridging bromide ligands were obtained from NMR scale experiments; several products were observed for La.[43] The synthesis of ligand precursor H_2LBr is facile and as a ligand should allow easy access for monomers to the rare-earth metal centre due to the small N-Me substituent; other fluorenyl tethered NHCs feature much larger aryl substituents.[23,24,45–47] These complexes will have high affinity for cyclic esters *via* the highly Lewis acidic/oxophilic rare-earth metal centres, the methyl NHC sidearm providing low steric hindrance and fluorenyl ring slippage to generate active sites at a higher rates.

The influence of steric hindrance in ligand sets is important in applications where reaction rate is of key importance. In the case of polymerisation this is especially true as the reaction is driven by ring strain energies (and thus propensity to ring-opening reactions) which vary significantly depending on the identity of the monomer.[12] Another well-known ligand type in rare earth chemistry is the scorpionate tris(1-pyrazolyl) borate (Tp^R) motif and the unsubstituted framework has been investigated recently by Farnaby and coworkers in bis(chelated) complexes of $[LnX(Tp)_2]$ (Ln = Y, Sm, Eu, Gd, Dy, Yb; X = OSO_2CF_3, N″ (N″ = $N(SiMe_3)_2$)).[48–52] Scorpionate complexes display significant steric bulk around the metal centre allowing direct comparisons in LA polymerisation between different ligand sets of the same metal type (Ln = Y) to be drawn where both feature an N″ coligand for initiation *via* reaction with BnOH. Herein, we report the synthesis and characterisation of several new bis(amide) Ln complexes bearing the fluorenyl-tethered NHC ligand $[Ln\{(\eta^5\text{-}C_{13}H_8)C_2H_4N(\kappa\text{-}C)C_2H_2N(Me)\}(N'')_2]$ ($LnLN''_2$; Ln = La, Ce, Nd) and the new heteroleptic amide bromide complex $[Ce\{(\eta^5\text{-}C_{13}H_8)C_2H_4N(\kappa\text{-}C)C_2H_2N(Me)\}(N'')(\mu\text{-}Br)]_2$. These complexes and those reported previously have been applied to the polymerisation of LA and display high reaction rates at room temperature while exhibiting a dependency on steric availability of the metal centres depending on the identity of the coligands.[43] We have also investigated $[Y(N'')Tp_2]$ in the polymerisation of LA and this highly hindered metal centre showed greatly reduced reaction rate.

Results and discussion

Synthesis

Previous work in the group has demonstrated the versatility of the fluorenyl-tethered N-heterocyclic carbene ligand, generated from the *N*-methyl imidazolium precursor $[(C_{13}H_9)C_2H_4N(CH)C_2H_2N(Me)][Br]$ (LH_2Br) in the synthesis of a range of metal complexes including lithium and rhodium.[23,24] The molecular structure of the imidazolium precursor was determined by X-ray diffraction experiments and reveals a fluorene group teth-

ered at C1 to a methylimidazolium ring by a C_2H_4 linker (Fig. 1). The full crystal structure features the bromide anion H-bonding to three different cations *via* H1 on the fluorene ring, H17 and H18, along with an interaction with C16 and H16 of another cation (see SI).

Direct reactions between $[Ln\{N(SiMe_3)_2\}_3]$ and LH_2Br in toluene allowed for the synthesis of complexes **1**–**4** (Scheme 1). Complex **4** was isolated on a preparative scale for the first time.[43] *In situ* double-deprotonation of the fluorene and imidazole moieties by two amide groups from the precursor allowed for complexation of L as a monoanionic chelating ligand together with incorporation of bromide as the final anionic ligand. The structures of the resulting complexes varied according to the ionic radius of the central metal atom. The Y complex **1** was obtained *via* crystallisation from toluene (38%) whereas the analogous reaction with La^{3+} – the largest rare-earth metal – undergoes ligand redistribution giving a mixture of products, **2** and **5**. Direct isolation of **2** was facilitated by its poor solubility in toluene which results in precipitation of the product as the reaction progresses. Further washing with toluene gave the impure product LaL_2Br (**2**) as a yellow powder. Cerium is the most abundant of the rare-earth elements making it an attractive target for complexation by reaction of CeN''_3 with LH_2Br.[53] As Ce is intermediate in ionic radius between La and Nd we were interested in whether the complex would show behaviour akin to La or Nd.[13] The Ce and Nd complexes (**3** and **4** respectively) were synthesised by the reaction of LnN''_3 in toluene with LH_2Br in a 1 : 1 molar ratio after stirring over 3 days at 80 °C. As the reaction proceeds, the insoluble product precipitates out of the solution allowing isolation of the product by cannula filtration followed by washing with toluene (**3**, orange powder, 71% or **4**, yellow powder, 51%).

Crystallisation of **3** from a C_6D_6 reaction mixture yielded orange plate crystals, shown by SCXRD to conform to the dimeric structure of **4**, hence yielding $[Ce\{(\eta^5\text{-}C_{13}H_8)C_2H_4N(\kappa\text{-}C)C_2H_2N(Me)\}(\mu\text{-}Br)N(SiMe_3)_2]_2$ (Fig. 2). Unfortunately, **3** and **4** cannot be redissolved after they have precipitated from the reaction mixture, so NMR spectroscopic data could not be recorded. However, reactions between CeN''_3 and LH_2Br in C_6D_6 on small scales allowed some ^1H NMR spectroscopic data to be acquired as some of the product is solvated upon formation (see SI).

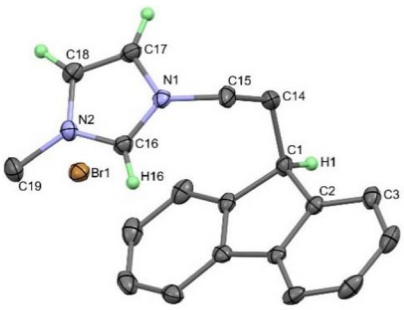

Fig. 1 Molecular structure of LH_2Br (thermal ellipsoids at 50%). For clarity, only selected H atoms are shown.

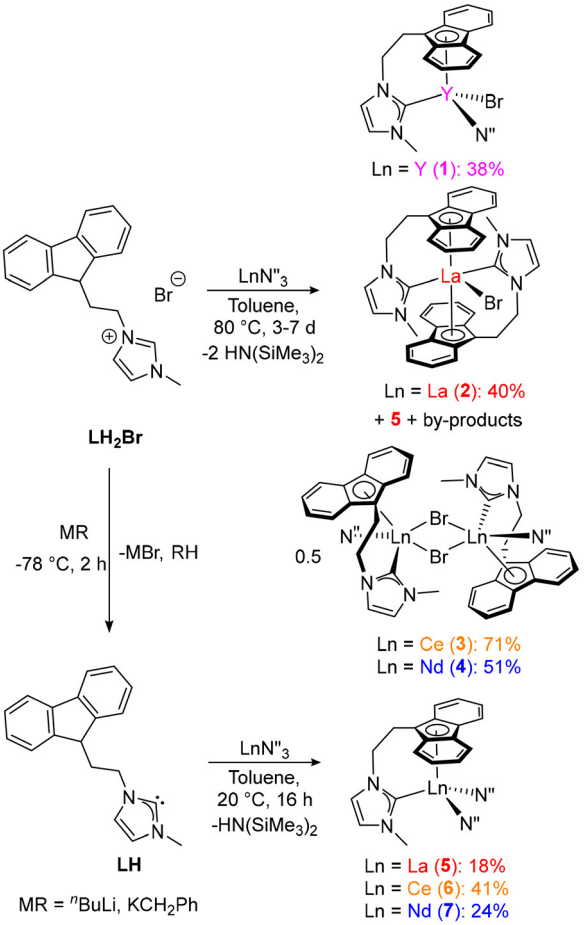

Scheme 1 Synthesis of heteroleptic rare-earth complexes.

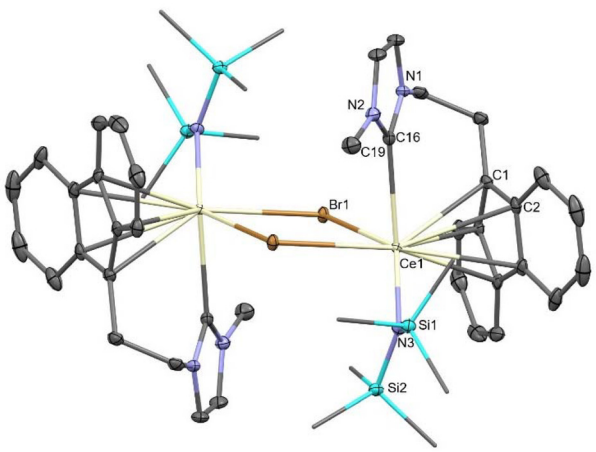

Fig. 2 Molecular structure of **3** determined by SCXRD. Thermal ellipsoids are at 50% probability with the carbon atoms of $SiMe_3$ groups set as capped sticks for clarity.

The dimeric bromide complexes **3** and **4** are insoluble in toluene and other common solvents such as MeCN and THF while chlorinated solvents risk chlorination of the com-

plexes.[54] By comparison, the mononuclear yttrium analogue **1** has good solubility in toluene. Therefore, synthesis of the analogous monomeric bis(amide) complexes with the form $LnLN''_2$ was sought to improve solubility as the $N(SiMe_3)_2$ (N″) group is well known for its solubilising properties. An alternative reaction methodology to selectively synthesise (bis)amide complexes was conveniently achieved by formation of the free carbene first *via* deprotonation of LH_2Br with one equivalent of ^{n}BuLi or KCH_2Ph at −78 °C (Scheme 1).[43] The imidazolium proton is the most acidic, thus deprotonation is exclusively from this site rather than the fluorenyl 9-H proton. As the MBr by-product is insoluble in toluene, the reaction mixture can then be filtered directly into a flask with the respective LnN''_3 precursor to initiate deprotonation of the Flu 9-H proton. The resulting synthesis of the bis(amide) complexes is significantly more facile than that of the bromide complexes, and reactions proceed well at room temperature for all three lanthanides when stirred for 16 hours.

Synthesis of the postulated yttrium (bis)amide complex (YLN''_2) was unsuccessful *via* the same route as complexes **5–7**; reaction of LH with YN''_3 at room temperature showed no deprotonation of the 9-H proton of the fluorenyl ring instead only showing resonances for the free carbene. Heating did not lead to clean formation of the desired complex, with several species observed lacking Y–C ^{13}C NMR resonances. Other routes investigated on small scales showed resonances inconsistent with those expected for the postulated complex indicating that steric constraints of the relatively small Y centre preclude a stable (bis)amide complex that also accommodates L.

Isolation of **5–7** was achieved by addition of hexane to a toluene solution of the reaction mixture. Once onset of precipitation was observed, the addition of hexane was stopped, and the reaction mixture was filtered and stored at −25 °C overnight to facilitate formation of large orange or yellow crystals, which were isolated by filtration. Purity was confirmed by ^{1}H and $^{13}C\{^1H\}$ NMR spectroscopy in the case of diamagnetic La while also being supported by elemental analyses for the other complexes.

Single crystals of compounds **5**, **6** and **7** suitable for X-ray diffraction analysis were obtained by storing saturated solutions of *ca.* 15 mg of the complex in hexane at −25 °C overnight. **5** has been previously reported by our group to show two molecules in the asymmetric unit ($P\bar{1}$) but the new data set showed one molecule ($Pca2_1$).[43] The structural data obtained confirmed the formation of the desired products ($LnLN''_2$) for all three lanthanides and showed that the complexes are isostructural. However, the crystallographic models for **5–7** showed large residual peaks next to the metal centres (see Table S2 in the SI), and thus they are presented as confirming the connectivity only. For **6** and **7**, the fluorenyl group is bound to the rare earth centre and the C_2H_4 tether to the carbene group then bends around to either the right or left to give enantiomers in the solid state (Fig. 3). The presence of a second N″ coligand bound to the metal centre results in greatly increased steric bulk around the metal compared to the bromide analogue **3** which is dimeric.

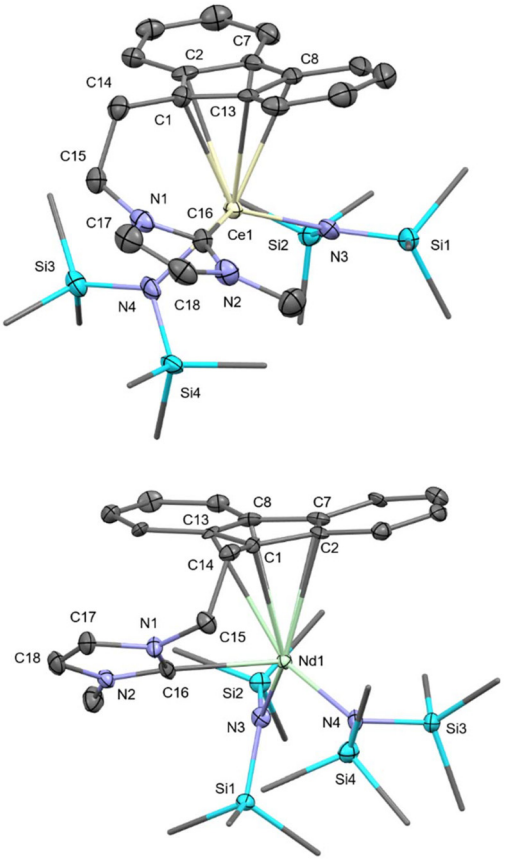

Fig. 3 Molecular structure of **6** (top) and **7** (bottom). Thermal ellipsoids are at 50% probability with the C atoms of the $SiMe_3$ groups set as capped sticks for clarity; all hydrogen atoms have been omitted.

rac-Lactide ring-opening polymerisation (ROP)

Note on ROP inhibition due to lactic acid contamination. During this study, several experiments unexpectedly resulted in poor conversions (≤30%) under conditions which previously would have yielded full consumption of LA. This was observed visually as the incomplete experiments display the remaining LA as an off-white suspension in contrast to the homogeneous and transparent solutions found with full conversion. Despite carefully following literature procedures for the purification of *rac*-lactide (*i.e.* recrystallisation from anhydrous toluene followed by triple sublimation under reduced pressure) the problematic batch of LA used was found to still be contaminated with significant quantities of lactic acid which can be observed in the methine region of the ^{1}H NMR spectrum (Fig. 4).

This contamination was on the order of 1.5% and this contaminant is particularly problematic as the catalyst species bear multiple basic sites which have the potential to react with the impurity and prevent full conversion of the monomer, particularly in cases of high monomer loading reported here. While these lactate complexes have not been intentionally synthesised, a postulated reaction scheme is shown below (Scheme 2). To ensure representative experimental data, results from polymerisation experiments presented in this

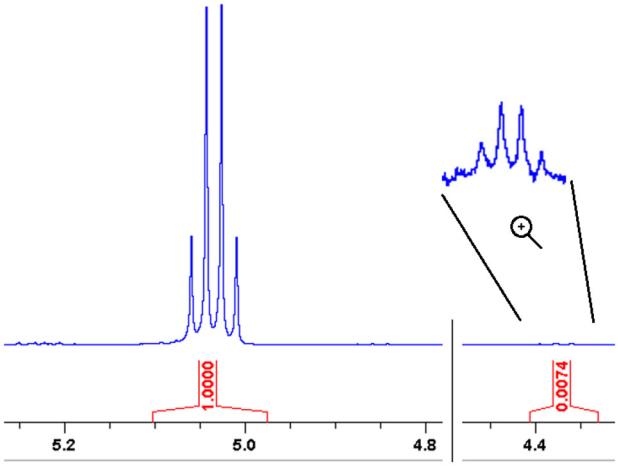

Fig. 4 ^{1}H NMR (400 MHz, $CDCl_3$, 298 K) spectrum of contaminated LA (left hand side) purified by literature procedures but maintaining lactic acid contamination (right hand side). N.B. A different batch of LA with minimal lactic acid contamination was used for polymerisation experiments shown in Table 1 – ^{1}H NMR spectrum of pure LA shown in Fig. S10.

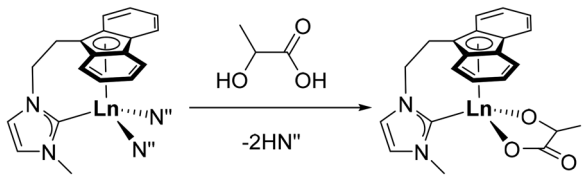

Scheme 2 $LnLN''_2$ catalyst poisoning by lactic acid.

study were obtained using LA purified from a batch verified to contain only negligible initial quantities of lactic acid contamination then purified according to literature procedures.

ROP of pure *rac*-LA

The potential of lanthanide complexes **1**, **3**–**7** to act as catalysts for the ROP of racemic lactide at ambient temperature with benzyl alcohol (BnOH) added to form alkoxide complexes *in situ* was tested. In each experiment, 1 mmol (*ca.* 144 mg) of *rac*-lactide was used and the total volume of solvent was made up to 2 mL to ensure constant conditions with respect to LA and the PLA product. BnOH was added as a standard solution in toluene (0.005 M) along with the chosen catalyst as either a powder dissolved/suspended in toluene (catalysts **1** **3**, **4**) or a standard solution of catalyst in toluene (catalysts **1**, **5**–**8**, 0.005 M; **8** = $[Y(N'')Tp_2]$). The complexes all showed high activity with full conversion typically being achieved in ≤15 minutes at 200 : 1 $[LA]_0$: [cat] loading. In all cases we did not observe any evidence of the catalyst exhibiting stereochemical control over the microstructure of the polymer formed. The polymer properties were determined by calibrated gel permeation chromatography (GPC) (Table 1). In addition to the primary polymer peaks observed in Table 1, a secondary minor peak of low M_w (unadjusted by Mark–Houwink parameters of roughly 600–800 g mol^{-1}, *i.e.* 4–6 monomer units) was observed in some reactions. We attribute these to the formation of cyclic PLA oligomers as a secondary product. Previous work from Arnold and coworkers has implicated amide and aryloxide tethered NHC catalysts in the production of cyclic PLA.[55,56] APCI mass spectrometry of polymer samples has revealed peaks close to the ideal value for short oligomers (see Fig. S33 and 34).

The catalysts featuring bromide co-ligands were poorly soluble in toluene with the exception of **1** and so the catalyst was added directly to the polymerisation vials as a solid powder rather than standard solutions. Despite the poor solubility of these pre-catalysts these reactions proceeded well and typically yielded a homogeneous transparent solution in reactions where full conversion was achieved. By this observation it appears that reaction of insoluble catalysts **3** and **4** with BnOH ($PhCH_2OH$) and LA forms species with markedly improved solubility allowing for reactions between catalysts and LA. It is noted that equimolar reactions of **1** and BnOH attempted on a small scale showed that several species exist in solution (see SI).

When catalyst **1** was added directly as a powder (entry 1), the polymer obtained showed the highest deviation from the calculated molecular weight at 35.1 kg mol^{-1} (M_n(calc) = 26.8 kg mol^{-1}). We attribute this to inefficient generation of the active species leading to longer polymers than expected while also broadening $Đ$. Of the Br complexes, **1** was the only catalyst that was readily soluble in toluene, so experiments as a 0.005 mmol mL^{-1} standard solution were also performed allowing for accurate loading up to 800 : 1 $[LA]_0$: [cat]. Reactions proceeded well with full conversion obtained in ≤10 minutes at 200 : 1 and ≤20 minutes at 400 : 1 while a 92% conversion was observed at 800 : 1 after 30 minutes. Control over polydispersity was good across all loadings, with the best value of 1.06 being obtained at 800 : 1 loading (entry 4). M_n varies across the loadings but was lower than M_n(calc) in all cases, while still exceeding those obtained at equivalent loadings using catalysts **3** and **4**. The 800 : 1 reaction produced polymer of shorter chain lengths than those from reactions at 400 : 1. Catalyst **3** reached full conversion within 15 minutes and had good control over $Đ$. The reaction generated shorter than calculated polymer chains indicating a prevalence of transesterification side-reactions or early termination reactions shortening polymer chains. Catalyst **3** showed a polydispersity of 1.36 while the M_n of 4.4 kg mol^{-1} was much smaller than the calculated value of 30.1 kg mol^{-1} suggesting that this initiator was more prone to transesterification side-reactions (entry 5).

Precatalyst **4** is dimeric but gave a narrow polydispersity at 1.31 and had the slowest reaction rate with only 78% conversion after fifteen minutes (entry 6). We attribute the slower rate of conversion to the small ionic radius of Nd which results in a more crowded active site and thus reduction of the rate *via* steric hindrance. A reaction without addition of benzyl alcohol (entry 7) showed that whilst the rate was not affected, the control over polymer properties was much worse. Only

Table 1 Data for the polymers formed from ROP of *rac*-lactide using catalysts **1**, **3–8**

Entry	Catalyst[a]	$[LA]_0:[cat]$	Time	Temp. (°C)	Conversion/%[b]	M_n(calc)[c]/kg mol^{-1}	M_n(exp)/kg mol^{-1}	M_w/kg mol^{-1}	$Đ$[d]
1	**1**	188	15 min	20	99	26.8	35.1	100.8	2.88
2	**1**[e]	200	10 min	20	99	28.4	11.6	16.2	1.39
3	**1**[e]	400	20 min	20	99	57.3	32.6	37.6	1.15
4	**1**[e]	800	30 min	20	92	106.0	30.3	32.1	1.06
5	**3**	211	15 min	20	99	30.1	4.4	5.9	1.36
6	**4**	194	15 min	20	78	21.8	53.1	70.2	1.31
7	**4**[f]	199	15 min	20	78	22.4	1.0	1.6	1.59
8	**5**[e]	200	10 min	20	99	28.7	18.9	25.3	1.33
9	**5**[e]	400	15 min	20	98	56.9	22.5	33.1	1.47
10	**6**[e]	200	5 min	20	99	28.6	12.8	17.7	1.38
11	**6**[e]	400	10 min	20	98	56.9	31.0	48.8	1.58
12	**7**[e]	200	10 min	20	99	28.6	21.0	32.9	1.56
13	**7**[e]	800	15 min	20	34	39.5	14.5	22.1	1.53
14	**8**[e]	200	30 min	20	5	—	—	—	—
15	**8**[e]	200	16 h	60	83	24.2	8.4	12.0	1.43
16	**8**[e]	400	16 h	60	63	36.6	20.7	21.6	1.05
17	**8**[e]	800	16 h	60	48	55.3	4.7	7.1	1.52
18	**8**[e]	200	16 h	80	93	26.8	7.6	9.5	1.26
19	**8**[e]	400	16 h	80	86	49.8	5.2	7.8	1.50
20	**8**[e]	800	16 h	80	80	92.2	7.8	11.6	1.48

[a] 1 : 1 ratio of benzyl alcohol added per metal centre. [b] Conversion calculated from integration of ^{1}H NMR spectra ($CDCl_3$) of crude reaction mixture aliquot, methine resonance at δ = 4.92 ppm for LA and δ = 5.00–5.30 ppm for PLA. [c] M_n(calc) obtained *via* (144.126 × $[LA]_0$/[cat] × % conversion). [d] $Đ$ = polydispersity index = M_w/M_n. [e] Catalyst added to reaction mixture as standard solution dissolved in toluene (0.005 mmol mL^{-1}). [f] Reaction performed without addition of benzyl alcohol.

short chain polymers were observed with an M_n of 1.0 kg mol^{-1} and a polydispersity of 1.59, suggesting that BnOH is necessary as the co-initiator to prevent early termination reactions.

The lanthanide bis(amide) complexes **5–7** showed good solubility in toluene and thus standard solutions could be made up for **5–7** and used directly in a 1 : 1 v : v ratio with a benzyl alcohol standard solution of equal concentration. Unlike catalysts **1**, **3** and **4**, where complex geometry varies greatly depending on the metal centre, **5–7** share the same structure across all three lanthanides. Direct comparisons can be drawn as the only variable is the size of the metal ion and so we expected relatively similar performance across the group, however, the results vary significantly both in control of polymer properties and in terms of reaction rate (Table 1).

Catalyst **5** showed very high activity, with 200 : 1 loading showing full conversion after 10 minutes (entry 8) and 98% conversion after 15 minutes at the higher 400 : 1 catalyst loading (entry 9). M_n is significantly lower than calculated for both 200 : 1 and 400 : 1 reactions, perhaps due to La(III) being the largest of the group and enabling greater steric freedom for side-reactions. The $Đ$ appears relatively well controlled (1.33 and 1.47), and the catalyst does not show evidence for degradation at the increased 400 : 1 loading.

6 (entries 10 and 11) exhibited the fastest reaction rate of all catalysts. Full conversion was achieved in only 5 minutes at 200 : 1 and can be extended in a linear fashion when monomer loading is increased to 400 : 1 where 98% conversion is observed in 10 minutes. M_n (12.8 kg mol^{-1}) shows the greatest discrepancy from M_n(calc) (28.6 kg mol^{-1}) among **5–7** indicating greater rates of transesterification side reactions but the degree is less compared to that observed when **3** was tested (M_n = 4.4 kg mol^{-1}, M_n(calc) = 27.4 kg mol^{-1}) which also features a Ce metal centre. At the increased 400 : 1 monomer loading the polymer displayed a broader $Đ$ relative to experiments at 200 : 1 (1.58 *vs.* 1.38) indicating a reduction in control as the initial concentration of monomer increases.

The Nd catalyst, **7**, polymerises lactide at a comparable rate to the other lanthanide catalysts achieving full conversion in 10 minutes at room temperature (entry 12). The $Đ$ of the purified polymer is slightly broader than others in the group at 1.56 but displayed good control over molecular weight with an M_n(exp) of 21.0 kg mol^{-1} *vs.* M_n(calc) of 28.6 kg mol^{-1} indicating only minor transesterification or other side reactions have occurred.

At high catalyst loadings, catalysts **5–7** appeared to be susceptible to degradation. Polymerisations at 800 : 1 catalyst loading frequently displayed incomplete conversions *ca.* 20–35% even with longer reaction times (entry 13). Comparison with the industrial PLA ROP catalyst, tin octoate, shows that the new fluorenyl-tethered NHC complexes **1**, **3–7** show improved rates with full conversion being obtained in shorter times and without external heating of the reaction mixture. Polydispersity of the synthesised polymers is typically ≤1.5 which is superior to that obtained from tin octoate (*ca.* 2.0)[57] while **1** shows a minimum polydispersity of 1.06 at the lowest loading. Molecular weights of the polymers obtained are typically below the M_n(calc) especially in the case of reactions with lower catalyst loadings (*i.e.* 800 : 1) while tin octoate shows higher tolerance for impurities at low catalyst loadings.

This paper represents the first fluorenyl-tethered NHC complexes investigated in ROP of *rac*-lactide but NHC complexes

tethered to other moieties have previously been synthesised and used such as alkoxide-tethered NHC cerium complexes in the Arnold group.[55] While the reaction rate of these cerium catalysts is better, the polydispersity of polymer obtained is higher showing a $Đ$ of 1.67 at 300 : 1 catalyst loading *versus* 1.38 at 200 : 1 and 1.58 at 400 : 1 for catalyst **6**. Other examples of yttrium catalysts, such as the benchmark phosphasalen complexes from the Williams group, show full conversion being obtained in as little as 5 seconds at the highest loadings.[58] These findings have not been matched here, however, control over polydispersity in this case can be improved as experiments using catalyst **1** show polydispersities matching or exceeding those from this study (1.06 for **1** *versus* 1.08–1.42).

YTp_2N'' complex (8)

Complex **8** bears two tris-pyrazolyl borate ligands and is found to be fully soluble in toluene, thus, as with **5–7**, standard solutions were utilised for the polymerisation experiments. Synthesis of the pre-catalyst is shown below (Scheme 3).

This ligand set is extremely bulky and thus steric hindrance to approach of the monomer during polymerisation experiments is significant and can clearly be implied by the need for additional heating in comparison to **1**, **3–7** to achieve significant conversions (Table 1, entries 14 and 15).

Initial experiments at room temperature showed only minor conversion <5% after 30 minutes, therefore, subsequent experiments were conducted with additional heating at 60 or 80 °C. At the elevated temperatures, stirring overnight was required to achieve reasonable conversions reaching a maximum of 83% at 60 °C and 93% at 80 °C (Fig. 5). As the concentration of LA decreases over the course of the reaction, in addition to an increase in viscosity of the reaction mixture, the reaction rate decreases. All reactions failed to reach full conversion after 16 hours at both 60 and 80 °C even at the 200 : 1 catalyst loading. In comparison, the steric effects of the two tris-pyrazolyl borate ligands appear to have far more effect than the tethered fluorenyl ligand in complexes **1**, **3–7** which generally reached full conversion without issue at room temperature and at shorter reaction times.

While **8** showed conversion of 83% at 200 : 1 catalyst loading (entry 15), reactions at higher loadings also proceed well, albeit at a slower rate indicating that the catalyst is tolerant to the increased reaction temperature. 60 °C reactions at 400 : 1 loading display a lower conversion at 63% while 800 : 1 is the lowest at 48% (entries 16 and 17); these values show that the relation between conversion and catalyst loading do not scale in a linear fashion. Control over M_n appears complex as

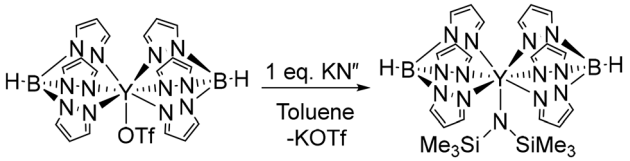

Scheme 3 Synthesis of $Y(Tp_2)N''$ from $Y(Tp)_2OTf$.

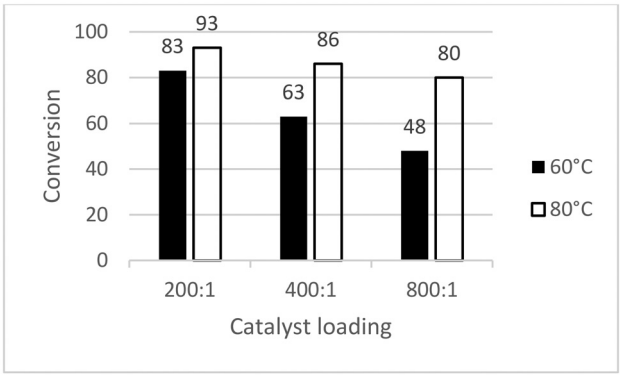

Fig. 5 Conversion of LA by **8** after 16 hours heating at 60 or 80 °C.

no trend in molecular weight and $Đ$ can be discerned from the GPC data which varies greatly among the different loadings.

Increasing the reaction temperature to 80 °C greatly improved the reaction kinetics as all three catalyst loadings are much closer to full conversion with the minimum conversion observed at 80% with 800 : 1 loading (Fig. 5). Higher loadings of catalyst also show increased conversion relative to 60 °C experiments with the same loading following the expected trend of increased conversion with increased energy input. The molecular weights of the polymers do not show agreement with M_n(calc) indicating premature chain cleavage as $Đ$ and M_n(exp) are on the same order for all three catalysts with some minor variations.

Comparison between the steric bulk of the three types of complexes [bromide (**1**, **3** and **4**), (bis)amide (**5–7**) and tris-pyrazolyl borate (**8**)] shows a clear influence on reaction rate. The two yttrium initiators (**1** and **8**) vary in steric hindrance in a clear manner which can be linked directly to reaction rate. **1** shows the least hindrance while achieving the fastest rate owing to its monomeric structure and small bromide ligand allowing access to the metal centre for the monomer. The Tp ligand presents a much greater steric constraint towards monomer binding, and this is reflected by the greatly reduced reaction rate. Bearing this in mind the use of the NHC-methyl pendant arm is likely to be important for catalysts **1**, **3–7** as more commonly larger *N* substituents are used with NHC ligands such as Dipp (diisopropylphenyl) or mesityl which present a much greater steric barrier to monomer binding. Tp is an even bulkier ligand and the extreme decrease in reaction rate relative to **1**, **3–7** suggests that this ligand is unsuitable for polymerisation catalysts at least in the case of yttrium.

Conclusion

Heteroleptic rare earth metal complexes (Ln = La, Ce, Nd) have been synthesised featuring a fluorenyl-tethered NHC ligand and applied to the ROP of *rac*-lactide. The Ce bromide complex **3** forms a dimeric species whereas the bis(amide) species are monomeric for all metal centres. **1** and **3–7** have proven to be

highly active catalysts for ROP without the need for external heating achieving full conversion of LA in as little as 5 minutes in the case of **6**. The reaction rate appears to be strongly linked to steric factors, with **8** in particular showing a significantly reduced reaction rate in comparison to the other Y species. Molecular weights of the synthesised polymers from the bromide catalysts varied depending on the identity of the metal – some lower than the M_n(calc) indicating transesterification reactions terminating chains prematurely while others are much larger than expected. The bis(amide) complexes typically generated polymer of more consistent chain lengths which were much closer, although still lower, than the M_n(calc). Control over polydispersity was generally greater than that of tin octoate with some reaching $Đ$ of *ca.* 1.1. Also of note is that the polymer obtained from reactions with complexes **1**, **3–8** was colourless in all cases. Additionally, the influence of lactic acid impurities and their ability to prevent full conversion by rapid degradation of catalysts to inactive species has been identified.

Experimental

Starting materials were used as received from Acros Organics, Alfa Aesar and Thermo Scientific. All NMR spectra were collected on a Bruker AVIIIHD 400 MHz spectrometer at 298 K at Heriot-Watt University. All manipulations were carried out under a dry, oxygen-free dinitrogen atmosphere using standard Schlenk line techniques or in an MBRAUN UNIlab glovebox. ^{1}H NMR spectra were recorded at 400 MHz and referenced to the residual solvent peak, 7.24 ppm for $CDCl_3$ and 7.16 ppm for C_6D_6. $^{13}C\{^1H\}$ NMR spectra were recorded at 101 MHz and referenced to the residual solvent peak, 128.06 ppm for C_6D_6. The size exclusion chromatography analysis of polymers was carried using a Shimadzu High Performance Liquid Chromatograph fitted with a 7.5 mm internal diameter Agilent GPC column. The detector used was a Shimadzu RID-20A. HPLC grade tetrahydrofuran (THF, 99.8%, Acros Organics, Geel, Belgium) was utilized as the eluent with a flow rate of 1 mL min^{-1} and an oven temperature of 30 °C. The measurement was calibrated against ten polystyrene standards in the range of 162–364 000 g mol^{-1} and corrected using the Mark–Houwink parameters, PLA (K = 0.0549, α = 0.639) and PS (K = 0.0125, α = 0.717).[59] Tetrahydrofuran (THF), acetonitrile and toluene were obtained from an MBRAUN SP-300 solvent purification system; further to this, toluene was boiled over molten sodium, then collected and stored over activated 4 Å molecular sieves. Dry diethyl ether was received in an AcroSeal bottle and was transferred to a new vessel and stored over 4 Å molecular sieves; residual gasses were then removed *via* 3 freeze–pump–thaw cycles. ^{n}BuLi was titrated three times with menthol and 2,2′-bipyridine. Elemental analysis was carried out by London Metropolitan University. Deuterated benzene was stirred over molten potassium and vacuum transferred prior to use. LH_2Br,[23] **1** [43] and **8** [48] were synthesised as previously described. $Ln\{N(SiMe_3)_2\}_3$ (Ln = Y, La, Ce, Nd) were synthesised from the reaction of anhydrous $LnCl_3$ salts with $NaN(SiMe_3)_2$ in THF, followed by toluene extraction and crystallisation.[60] *rac*-Lactide was purified by recrystallisation from toluene followed by triple sublimation prior to use, however, only *rac*-lactide that was free of lactic acid impurity when purchased was used for polymerisation experiments, as verified by ^{1}H NMR spectroscopy.

[LnL(N″)(Br)]$_2$ & LaL$_2$Br (2, 3, 4)

[9-($C_{13}H_9$)C_2H_4N(CH)C_2H_2N(Me)][Br] (0.1153 g, 0.325 mmol) and $Ln(N(SiMe_3)_2)_3$ (0.325 mmol) were added to a Schlenk flask in the glovebox. Dry toluene (10 mL) was also added, and the resulting mixture was stirred at room temperature for 30 minutes then at 80 °C (La = 3 d, Ce = 16 h, Nd = 3 d). Over the course of the reaction the products precipitate as yellow or orange solids. The reaction was cooled to room temperature and the volatile components are then removed under reduced pressure. The resulting yellow or orange solids are washed with toluene (10 mL) and dried under reduced pressure. LaL$_2$Br (**2**): (0.1154 g, 0.151 mmol, 40%) (CeLN″Br)$_2$ (**3**): (0.1514 g, 0.116 mmol, 71%), (NdLN″Br)$_2$ (**4**): (0.1085 g, 0.0825 mmol, 51%). Analysis calculated for **3**: C 45.93, H 5.40, N 6.43, found: C 44.07, H 5.07, N 5.31. Analysis calculated for **4**: C 45.64, H 5.36, N 6.39, found: C 45.86, H 4.11, N 5.40.

LnLN″$_2$ (Ln = La, Ce, Nd) (5, 6, 7)

[9-($C_{13}H_9$)C_2H_4N(CH)C_2H_2N(Me)][Br] (0.590 g, 1.66 mmol) and toluene (20 mL) were added to an ampoule equipped with J. Youngs tap in the glovebox. To this suspension was added ^{n}BuLi (0.98 mL, 1.64 M, 1.60 mmol) at −78 °C, then the reaction was left to warm to room temperature and was stirred for 16 hours. The stirring was stopped, the LiBr in solution was left to settle and the free carbene was transferred to another Schlenk flask containing $[Ln\{N(SiMe_3)_2\}_3]$ (1.60 mmol) dissolved in dry toluene (20 mL) *via* cannula filtration. The resulting solution was then stirred for 16 hours at room temperature. The solution was then filtered, and the resulting filtrate was dried under reduced pressure with slight heating to remove $HN(SiMe_3)_2$. The resulting solids were redissolved in toluene (10 mL) and dry hexane or pentane (30 mL) was added until a precipitate was observed. The solution was filtered and the filtrate stored at −25 °C to induce crystallization of the product, which was isolated by filtration and dried under vacuum. LaLN″$_2$ (**5**) (0.2171 g, 0.296 mmol, 18%), CeLN″$_2$ (**6**) (0.4941 g, 0.673 mmol, 41%), NdLN″$_2$ (**7**) (0.2970 g, 0.402 mmol, 24%).

5: ^{1}H NMR (400 MHz, 298 K, C_6D_6) δ (ppm): 8.19 (2H, d, J = 8.0 Hz, H_{Flu}), 7.11 (4H, m, H_{Flu}), 6.71 (2H, br. s, H_{Flu}), 6.13 (1H, d, J = 1.6 Hz, NHC C*H*NCH$_2$), 5.94 (1H, d, J = 1.6 Hz, NHC C*H*NMe), 3.97 (2H, m, NCH$_2$), 3.06 (3H, s, Me), 2.95 (2H, m, CH$_2$), 0.19 (36H, s, N″); $^{13}C\{^1H\}$ NMR (101 MHz, 298 K, C_6D_6) (see SI for carbon labels) δ/ppm: 136.67 (C, C_{Flu}), 129.38 (C, C_{Flu}), 128.71 (C, C_{Flu}), 124.71 (C, C_{Flu}), 123.93 (C, C_{Flu}), 121.65 (C, C_{Flu}), 121.66 (C, C_q), 121.11 (C, C_{Flu}), 120.71 (C, C_r), 94.41 (C, C_a), 53.11 (C, C_o), 38.03 (C, C_s), 27.81 (C, C_n), 5.69 (C, C_t;

see SI for labelling); analysis calculated: C 50.80, H 7.29, N 7.64; found: C 51.09, H 7.24, N 7.30.

6: ^{1}H (400.1 MHz, 298 K, C_6D_6) δ/ppm: 14.86 (br. s, 1H, NHC_{CH}), 9.14 (br. s, 1H, NHC_{CH}), 5.84 (br. s, 2H, CH_2), 2.95 (br. s, 2H, CH_2), −3.69 (br. s, 36H, N″); analysis calculated: C 50.71, H 7.28, N 7.63; found: C 50.74, H 7.06, N 7.41.

7: ^{1}H (400.1 MHz, 298 K, C_6D_6) δ/ppm: 7.64 (d, 2H, H_{Flu}), 7.03 (br. s, 14H, H_{Flu}), 5.40 (d, 1H), 4.33 (s, 1.6H, H_o), 3.84 (d, 1H), 1.70 (s, 1H), 1.25 (s, 2H, CH_2), 0.89 (s, 2H, CH_2), 0.29 (s, 1H), −0.47 (s, 3H, Me), −3.18 (br. S, 36H, N″); analysis calculated: C 50.34, H 7.24, N 7.59; found: C 50.76, H 6.81, N 6.54.

General polymerisation protocol

A 7 mL vial with threaded PTFE lined cap was charged with *rac*-lactide (144.1 mg ± 1%, 1 mmol), a standard solution of benzyl alcohol in toluene (0.005 mmol mL^{-1}, 200 : 1 catalyst loading = 1 mL, 400 : 1 = 0.5 mL, 800 : 1 = 0.25 mL, equimolar to moles of catalyst) and toluene (200 : 1 catalyst loading = 0 mL, 400 : 1 = 1 mL, 800 : 1 = 1.5 mL). Insoluble bromide catalysts (**3**, **4**) were weighed (*ca.* 3–4 mg, 0.005 mmol by metal centre) and added as a suspension in toluene to the vial with *rac*-lactide whilst lanthanide (bis)amide catalysts (**1**, **5**, **6**, **7** and **8**) were added in solution with toluene (0.005 mmol mL^{-1}, 200 : 1 catalyst loading = 1 mL, 400 : 1 = 0.5 mL, 800 : 1 = 0.25 mL, equimolar to moles of benzyl alcohol). T = 0 is defined as the moment when catalyst is added to the reaction mixture. The vials are then stirred for the desired time. Following this, a crude sample is taken to determine conversion by ^{1}H NMR analysis and the reaction mixture is added to ice cold acidified methanol to quench the reaction. The sample was then frozen overnight at −25 °C and the methanol layer was decanted followed by drying at 50 °C in a vacuum oven to purify the samples for GPC analysis.

The full GPC traces for each experiment are shown in the SI.

Conflicts of interest

The authors declare no conflict of interest.

Data availability

The data supporting this article have been included as part of the SI.

Supplementary information: NMR spectroscopic and SCXRD characterisation of the complexes; additional polymerisation details and spectra. See DOI: **https://doi.org/10.1039/d5dt01352f**.

CCDC 2401175–2401179 contain the supplementary crystallographic data for this paper.[61a–e]

Acknowledgements

JWW thanks EaSI-cat for funding, and the Royal Society of Chemistry for a travel grant. TC and JHF thank the University of Glasgow (UoG) for funding, and the College of Science and Engineering (UoG) for the award of a PhD Scholarship to TC.

References

1 A. B. Kremer and P. Mehrkhodavandi, *Coord. Chem. Rev.*, 2019, **380**, 35–57.
2 H. Liu, F. You, X. Hu, Y. Huo and X. Shi, *Organometallics*, 2022, **41**, 3645–3653.
3 E. Fazekas, P. A. Lowy, M. Abdul Rahman, A. Lykkeberg, Y. Zhou, R. Chambenahalli and J. A. Garden, *Chem. Soc. Rev.*, 2022, **51**, 8793–8814.
4 D. M. Lyubov, A. O. Tolpygin and A. A. Trifonov, *Coord. Chem. Rev.*, 2019, **392**, 83–145.
5 C. Bakewell, T.-P.-A. Cao, N. Long, X. F. Le Goff, A. Auffrant and C. K. Williams, *J. Am. Chem. Soc.*, 2012, **134**, 20577–20580.
6 D. J. Ward, D. J. Saccomando, G. Walker and S. M. Mansell, *Catal. Sci. Technol.*, 2023, **13**, 2638–2647.
7 T. Goto, M. Kishita, Y. Sun, T. Sako and I. Okajima, *Polymers*, 2020, **12**, 2434.
8 A. Theodorou, V. Raptis, C. I. Baltzaki, T. Manios, V. Harmandaris and K. Velonia, *Polymers*, 2023, **15**, 4569.
9 D. J. Walsh, M. G. Hyatt, S. A. Miller and D. Guironnet, *ACS Catal.*, 2019, **9**, 11153–11188.
10 A. Schindler, Y. M. Hibionada and C. G. Pitt, *J. Polym. Sci., Polym. Chem. Ed.*, 1982, **20**, 319–326.
11 W. A. Munzeiwa, B. O. Omondi and V. O. Nyamori, *Polym. Bull.*, 2024, **81**, 9419–9464.
12 R. H. Platel, A. J. P. White and C. K. Williams, *Inorg. Chem.*, 2011, **50**, 7718–7728.
13 R. Shannon, *Acta Crystallogr., Sect. A: Found. Crystallogr.*, 1976, **32**, 751–767.
14 S. M. Mansell and S. T. Liddle, *Inorganics*, 2016, **4**, 31.
15 R. E. Cramer, J. M. Rimsza and T. J. Boyle, *Inorg. Chem.*, 2022, **61**, 6120–6127.
16 E. Kirillov, J.-Y. Saillard and J.-F. Carpentier, *Coord. Chem. Rev.*, 2005, **249**, 1221–1248.
17 F. Pammer and W. R. Thiel, *Coord. Chem. Rev.*, 2014, **270–271**, 14–30.
18 M. J. Calhorda and L. F. Veiros, *Comments Inorg. Chem.*, 2001, **22**, 375–391.
19 M. E. Rerek, L.-N. Ji and F. Basolo, *J. Chem. Soc., Chem. Commun.*, 1983, 1208–1209.
20 L. F. Veiros, *Organometallics*, 2000, **19**, 3127–3136.
21 C. Müller, D. Vos and P. Jutzi, *J. Organomet. Chem.*, 2000, **600**, 127–143.
22 M. Roselló-Merino and S. M. Mansell, *Dalton Trans.*, 2016, **45**, 6282–6293.
23 K. J. Evans, C. L. Campbell, M. F. Haddow, C. Luz, P. A. Morton and S. M. Mansell, *Eur. J. Inorg. Chem.*, 2019, **2019**, 4894–4901.
24 K. J. Evans, P. A. Morton, C. Luz, C. Miller, O. Raine, J. M. Lynam and S. M. Mansell, *Chem. – Eur. J.*, 2021, **27**, 17824–17833.

25 B. Royo and E. Peris, *Eur. J. Inorg. Chem.*, 2012, **2012**, 1309–1318.
26 D. J. Nelson and S. P. Nolan, in *N-Heterocyclic Carbenes*, 2014, pp. 1–24.
27 P. L. Arnold and I. J. Casely, *Chem. Rev.*, 2009, **109**, 3599–3611.
28 S. S. Bera and M. Szostak, *ACS Catal.*, 2022, **12**, 3111–3137.
29 G. G. Zámbó, J. F. Schlagintweit, R. M. Reich and F. E. Kühn, *Catal. Sci. Technol.*, 2022, **12**, 4940–4961.
30 M. Jalal, B. Hammouti, R. Touzani, A. Aouniti and I. Ozdemir, *Mater. Today: Proc.*, 2020, **31**, S122–S129.
31 M. Scholl, S. Ding, C. W. Lee and R. H. Grubbs, *Org. Lett.*, 1999, **1**, 953–956.
32 D. McGuinness, *Dalton Trans.*, 2009, 6915–6923.
33 I. Jain and P. Malik, *Eur. Polym. J.*, 2021, **150**, 110412.
34 R. H. Crabtree, *J. Organomet. Chem.*, 2005, **690**, 5451–5457.
35 M. Konkol, T. P. Spaniol, M. Kondracka and J. Okuda, *Dalton Trans.*, 2007, 4095–4102.
36 C. Hermans, W. Rong, T. P. Spaniol and J. Okuda, *Dalton Trans.*, 2016, **45**, 8127–8133.
37 T. Zeng, Q. Qian, B. Zhao, D. Yuan, Y. Yao and Q. Shen, *RSC Adv.*, 2015, **5**, 53161–53171.
38 W. Li, Z. Zhang, Y. Yao, Y. Zhang and Q. Shen, *Organometallics*, 2012, **31**, 3499–3511.
39 Y. Luo, X. Wang, J. Chen, C. Luo, Y. Zhang and Y. Yao, *J. Organomet. Chem.*, 2009, **694**, 1289–1296.
40 B. Liu, D. Cui, J. Ma, X. Chen and X. Jing, *Chem. – Eur. J.*, 2007, **13**, 834–845.
41 Y. Yang, S. Li, D. Cui, X. Chen and X. Jing, *Organometallics*, 2007, **26**, 671–678.
42 M. A. Sinenkov, G. K. Fukin, A. V. Cherkasov, N. Ajellal, T. Roisnel, F. M. Kerton, J.-F. Carpentier and A. A. Trifonov, *New J. Chem.*, 2011, **35**, 204–212.
43 K. J. Evans, P. A. Morton, C. Sangster and S. M. Mansell, *Polyhedron*, 2021, **197**, 115021.
44 S. Li, D. Liu, Z. Wang and D. Cui, *ACS Catal.*, 2018, **8**, 6086–6093.
45 S. P. Downing, P. J. Pogorzelec, A. A. Danopoulos and D. J. Cole-Hamilton, *Eur. J. Inorg. Chem.*, 2009, **2009**, 1816–1824.
46 S. P. Downing and A. A. Danopoulos, *Organometallics*, 2006, **25**, 1337–1340.
47 S. P. Downing, S. C. Guadaño, D. Pugh, A. A. Danopoulos, R. M. Bellabarba, M. Hanton, D. Smith and R. P. Tooze, *Organometallics*, 2007, **26**, 3762–3770.
48 T. Chowdhury, S. J. Horsewill, C. Wilson and J. H. Farnaby, *Aust. J. Chem.*, 2022, **75**, 660–675.
49 T. Chowdhury, M. J. Evans, M. P. Coles, A. G. Bailey, W. J. Peveler, C. Wilson and J. H. Farnaby, *Chem. Commun.*, 2023, **59**, 2134–2137.
50 T. Chowdhury, C. Wilson, C. Maichle-Mössmer, R. Anwander and J. H. Farnaby, *Eur. J. Inorg. Chem.*, 2024, **27**, e202300731.
51 T. Chowdhury, C. Wilson and J. H. Farnaby, *Dalton Trans.*, 2024, **53**, 11884–11894.
52 T. Chowdhury, F. Murphy, A. R. Kennedy, C. Wilson, J. H. Farnaby and C. E. Weetman, *Inorg. Chem.*, 2024, **63**, 9390–9394.
53 A. A. Yaroshevsky, *Geochem. Int.*, 2006, **44**, 48–55.
54 M. S. Platz, *J. Phys. Org. Chem.*, 2024, **37**, e4563.
55 R. W. F. Kerr, P. M. D. A. Ewing, S. K. Raman, A. D. Smith, C. K. Williams and P. L. Arnold, *ACS Catal.*, 2021, **11**, 1563–1569.
56 D. Patel, S. T. Liddle, S. A. Mungur, M. Rodden, A. J. Blake and P. L. Arnold, *Chem. Commun.*, 2006, 1124–1126.
57 H. R. Kricheldorf and S. M. Weidner, *Polym. Chem.*, 2020, **11**, 5249–5260.
58 T.-P.-A. Cao, A. Buchard, X. F. Le Goff, A. Auffrant and C. K. Williams, *Inorg. Chem.*, 2012, **51**, 2157–2169.
59 P. Dubois, C. Jacobs, R. Jerome and P. Teyssie, *Macromolecules*, 1991, **24**, 2266–2270.
60 W. A. Herrmann and F. T. Edelmann, *Synthetic Methods of Organometallic and Inorganic Chemistry: Lanthanides and Actinides*, Thieme Medical Pub, 1996.
61 (*a*) J. W. Walker, T. Chowdhury, G. M. Rosair, J. H. Farnaby, S. M. Mansell and R. D. McIntosh, CCDC 2401175: Experimental Crystal Structure Determination, 2025, DOI: **10.5517/ccdc.csd.cc2llm83**; (*b*) J. W. Walker, T. Chowdhury, G. M. Rosair, J. H. Farnaby, S. M. Mansell and R. D. McIntosh, CCDC 2401176: Experimental Crystal Structure Determination, 2025, DOI: **10.5517/ccdc.csd.cc2llm94**; (*c*) J. W. Walker, T. Chowdhury, G. M. Rosair, J. H. Farnaby, S. M. Mansell and R. D. McIntosh, CCDC 2401177: Experimental Crystal Structure Determination, 2025, DOI: **10.5517/ccdc.csd.cc2llmb5**; (*d*) J. W. Walker, T. Chowdhury, G. M. Rosair, J. H. Farnaby, S. M. Mansell and R. D. McIntosh, CCDC 2401178: Experimental Crystal Structure Determination, 2025, DOI: **10.5517/ccdc.csd.cc2llmc6**; (*e*) J. W. Walker, T. Chowdhury, G. M. Rosair, J. H. Farnaby, S. M. Mansell and R. D. McIntosh, CCDC 2401179: Experimental Crystal Structure Determination, 2025, DOI: **10.5517/ccdc.csd.cc2llmd7**.